

Monopole Dominance of Confinement in SU(3) Lattice QCD

Hideo Suganuma*,

*Department of Physics & Division of Physics and Astronomy, Graduate School of Science,
Kyoto University, Kitashirakawaoiwake, Sakyo, Kyoto 606-8502, Japan
E-mail: suganuma@scphys.kyoto-u.ac.jp*

Naoyuki Sakumichi

Ochanomizu University, 2-1-1 Otsuka, Bunkyo, Tokyo 112-8610, Japan

To check the dual superconductor picture for the quark-confinement mechanism, we evaluate monopole dominance as well as Abelian dominance of quark confinement for both quark-antiquark ($Q\bar{Q}$) and three-quark (3Q) systems in SU(3) quenched lattice QCD in the maximally Abelian (MA) gauge. First, we examine Abelian dominance for the static $Q\bar{Q}$ system in lattice QCD with various spacing a at $\beta = 5.8 - 6.4$ and various size $L^3 \times L_t$. For large physical-volume lattices with $La \geq 2\text{fm}$, we find *perfect Abelian dominance* of the string tension for the $Q\bar{Q}$ systems: $\sigma_{\text{Abel}} \simeq \sigma$. Second, we accurately measure the static 3Q potential for more than 300 different patterns of 3Q systems with 1000-2000 gauge configurations using two large physical-volume lattices: $(\beta, L^3 \times L_t) = (5.8, 16^3 \times 32)$ and $(6.0, 20^3 \times 32)$. For all the distances, the static 3Q potential is found to be well described by the Y-Ansatz, i.e., two-body Coulomb term plus three-body Y-type linear term σL_{min} , where L_{min} is the minimum flux-tube length connecting the three quarks. We find *perfect Abelian dominance* of the string tension also for the 3Q systems: $\sigma_{3Q}^{\text{Abel}} \simeq \sigma_{3Q} \simeq \sigma$. Finally, we accurately investigate monopole dominance in SU(3) lattice QCD at $\beta=5.8$ on $16^3 \times 32$ with 2,000 gauge configurations. Abelian-projected QCD in the MA gauge has not only the color-electric current j^μ but also the color-magnetic monopole current k^μ , which topologically appears. By the Hodge decomposition, the Abelian-projected QCD system can be divided into the monopole part ($k_\mu \neq 0, j_\mu = 0$) and the photon part ($j_\mu \neq 0, k_\mu = 0$). We find monopole dominance of the string tension for $Q\bar{Q}$ and 3Q systems: $\sigma_{\text{Mo}} \simeq 0.92\sigma$. While the photon part has almost no confining force, the monopole part almost keeps the confining force.

*The XIIIth Quark Confinement and the Hadron Spectrum,
31 July - 6 August 2018
Maynooth University, Maynooth, Ireland*

*Speaker.

1. Introduction: Dual Superconductor Picture and Maximally Abelian Gauge

Quantum chromodynamics (QCD) is the fundamental theory of the strong interaction, but the QCD system is highly complicated and is still unsolved analytically because of its strong coupling in the low-energy region. In particular, quark confinement is an outstanding strange phenomenon exhibited in nonperturbative QCD, because the fundamental degrees of freedom, quarks and gluons, cannot be observed, and there is almost no similar phenomenon in other region of physics. In fact, to clarify the confinement mechanism is one of the most difficult important unsolved problems remaining in modern physics.

For the quark-confinement mechanism, Nambu, 't Hooft and Mandelstam proposed a dual-superconductor picture in 1970's [1]. In this picture, the QCD vacuum is regarded as a color-magnetic monopole condensed system, and the dual Meissner effect forces the color-electric flux between (anti)quarks to be squeezed into one dimension, which leads to the flux-tube picture of hadrons [2, 3]. However, there are two large gaps between QCD and the dual-superconductor picture [4].

1. The dual-superconductor picture is based on the Abelian gauge theory subject to the Maxwell-type equations, but QCD is a non-Abelian gauge theory.
2. The dual-superconductor picture needs color-magnetic monopole condensation as the key concept, but QCD does not have such a monopole as the elementary degrees of freedom.

As a possible connection from QCD to the dual superconductor picture, 't Hooft proposed "Abelian projection" [2, 3] as an infrared Abelianization scheme of QCD. In the Abelian projection, magnetic monopoles topologically appear, and 't Hooft conjectured that long-distance physics like confinement is realized only by Abelian degrees of freedom in QCD [2], which is called "(infrared) Abelian dominance".

Actually, in the maximally Abelian (MA) gauge [5], off-diagonal gluons acquire a large effective mass of about 1GeV [6], which makes infrared QCD Abelian-like [7], and lattice QCD shows appearance of a large clustering of the monopole current covering the four-dimensional space-time [5, 8]. In fact, infrared QCD in the MA gauge seems to behave as an Abelian dual-superconductor.

In $SU(3)$ lattice QCD, MA gauge fixing [9, 10] is performed by maximizing

$$R_{\text{MA}}[U_\mu(s)] \equiv \sum_s \sum_{\mu=1}^4 \text{tr} \left(U_\mu^\dagger(s) \vec{H} U_\mu(s) \vec{H} \right) = \frac{1}{2} \sum_s \sum_{\mu=1}^4 \left(\sum_{i=1}^3 |U_\mu(s)_{ii}|^2 - 1 \right), \quad (1.1)$$

under $SU(3)$ gauge transformation. Here, $U_\mu(s)$ is the link-variable $U_\mu(s) = e^{iagA_\mu(s)} \in SU(3)_c$ with lattice spacing a , gauge coupling g and gluon fields A_μ .

The Abelian link-variable $u_\mu(s) = e^{i\theta_\mu(s)} = e^{i\theta_\mu^3(s)T_3 + i\theta_\mu^8(s)T_8} \in U(1)^2$ is extracted from the link-variable $U_\mu^{\text{MA}}(s) \in SU(3)_c$ in the MA gauge [10], by maximizing the overlap of $R_{\text{Abel}} \equiv \frac{1}{3} \text{Re tr} \left(U_\mu^{\text{MA}}(s) u_\mu^\dagger(s) \right) \in [-\frac{1}{2}, 1]$. Maximally Abelian projection is defined by the replacement of $\{U_\mu^{\text{MA}}(s)\} \rightarrow \{u_\mu(s)\}$, which corresponds to the elimination of off-diagonal gluon components.

In this paper, to check the dual superconductor picture, we accurately investigate Abelian dominance [9, 10] and monopole dominance of the quark confining force for both quark-antiquark ($Q\bar{Q}$) and three-quark ($3Q$) systems in $SU(3)$ quenched lattice QCD in the MA gauge. For the error estimate, we use the jackknife method.

2. Perfect Abelian dominance of quark confinement in quark-antiquark systems

First, we study the static $Q\bar{Q}$ potential $V(r)$ in lattice QCD with $(\beta, L^3 \times L_t) = (6.4, 32^4), (6.0, 32^4)$ and $(5.8, 16^3 \times 32)$ [9, 10]. The $Q\bar{Q}$ potential $V(r)$ is obtained with the Wilson loop $W_{r \times t}[U_\mu]$, and its MA projection (Abelian part) $V_{\text{Abel}}(r)$ is similarly defined by the Abelian Wilson loop $W_{r \times t}[u_\mu]$,

$$V(r) = -\lim_{t \rightarrow \infty} \frac{1}{t} \ln \langle W_{r \times t}[U_\mu] \rangle, \quad V_{\text{Abel}}(r) = -\lim_{t \rightarrow \infty} \frac{1}{t} \ln \langle W_{r \times t}[u_\mu] \rangle. \quad (2.1)$$

We show in Fig.1(a) the $Q\bar{Q}$ potential $V(r)$ and its Abelian part $V_{\text{Abel}}(r)$. They are found to be well reproduced by the Coulomb-plus-linear Ansatz, respectively:

$$V(r) = -\frac{A}{r} + \sigma r + C, \quad V_{\text{Abel}}(r) = -\frac{A_{\text{Abel}}}{r} + \sigma_{\text{Abel}} r + C_{\text{Abel}}. \quad (2.2)$$

Figure 1(b) shows the difference $V(r) - V_{\text{Abel}}(r)$ plotted with r at each lattice. As a remarkable fact from Fig.1, we find *perfect Abelian dominance* of the string tension, $\sigma_{\text{Abel}} \simeq \sigma$, for the $Q\bar{Q}$ system.

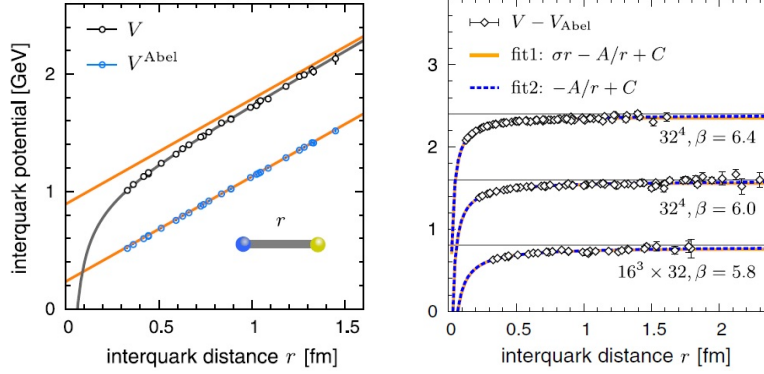


Figure 1: (a) The lattice QCD result of the $Q\bar{Q}$ potential $V(r)$ (black) and its Abelian part $V_{\text{Abel}}(r)$ (blue) for $(\beta, L^3 L_t) = (5.8, 16^3 32)$ [10]. (b) $V(r) - V_{\text{Abel}}(r)$ for $(\beta, L^3 L_t) = (6.4, 32^4), (6.0, 32^4)$ and $(5.8, 16^3 32)$ [9]. At each lattice, all the data can be well fit with the pure Coulomb form with $\sigma = 0$, which means $\sigma_{\text{Abel}} \simeq \sigma$.

We also examine the physical lattice-volume dependence of $\sigma_{\text{Abel}}/\sigma$ in Fig.2, and find perfect Abelian dominance ($\sigma_{\text{Abel}} \simeq \sigma$), when the spatial size La is larger than about 2 fm.

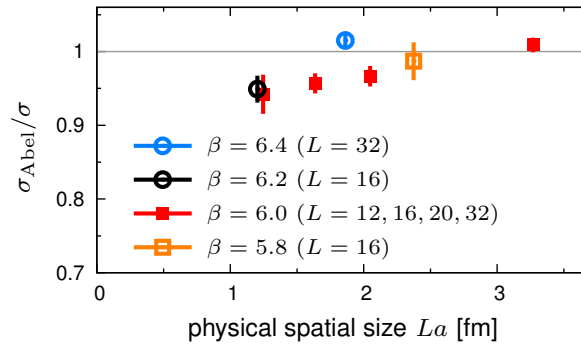


Figure 2: Physical spatial-size dependence of the ratio $\sigma_{\text{Abel}}/\sigma$ [10]. Perfect Abelian dominance ($\sigma_{\text{Abel}} \simeq \sigma$) is found for larger lattices with $La \geq 2$ fm.

3. Quark Confinement in Baryons

Second, we accurately measure the static three-quark (3Q) potential V_{3Q} [10] for more than 300 different patterns of 3Q systems with 1000-2000 gauge configurations in SU(3) lattice QCD on large physical-volume lattices with $La > 2\text{fm}$: $(\beta, L^3 \times L_t) = (5.8, 16^3 \times 32)$ and $(6.0, 20^3 \times 32)$.

3.1 Accurate Measurement of Three-Quark Potential

Like the $Q\bar{Q}$ potential, the 3Q potential V_{3Q} is obtained from the ‘‘3Q Wilson loop’’ W_{3Q} (an extension of the Wilson loop for gauge-invariant static 3Q systems) defined in Ref.[11]:

$$V_{3Q} = -\lim_{t \rightarrow \infty} \frac{1}{t} \ln \langle W_{3Q} [U_\mu] \rangle. \quad (3.1)$$

We consider 101 and 211 different patterns of 3Q systems with 2000 and 1000 gauge configurations at $\beta=5.8$ and 6.0, respectively. For the accurate calculation of the 3Q potential with finite t , we use the gauge-invariant smearing method [11], which enhances the ground-state component in the 3Q state in $\langle W_{3Q} \rangle$.

As the result, all the lattice QCD data of the 3Q potential V_{3Q} is found to be fairly well reproduced by the Y-Ansatz [10, 11], i.e., one-gluon-exchange Coulomb plus Y-type linear potential,

$$V_{3Q}(\mathbf{r}_1, \mathbf{r}_2, \mathbf{r}_3) = -\sum_{i < j} \frac{A_{3Q}}{|\mathbf{r}_i - \mathbf{r}_j|} + \sigma_{3Q} L_{\min} + C_{3Q} = -\frac{A_{3Q}}{R} + \sigma_{3Q} L_{\min} + C_{3Q}, \quad (3.2)$$

with $\sigma_{3Q} \simeq \sigma$ ($Q\bar{Q}$ string tension). L_{\min} is the minimal flux-tube length connecting the three quarks, located at $\mathbf{r}_1, \mathbf{r}_2$ and \mathbf{r}_3 . We here introduce a convenient variable $1/R \equiv \sum_{i < j} 1/|\mathbf{r}_i - \mathbf{r}_j|$ [12]. The Y-Ansatz (3.2) indicates the Y-shaped flux-tube formation in baryons, which is actually observed in lattice QCD calculations on the action density in the presence of three static quarks [13].

3.2 Perfect Abelian dominance of quark confinement in baryons

Next, we examine Abelian dominance of quark confinement in the 3Q system. Like the $Q\bar{Q}$ case, the MA-projected 3Q potential V_{3Q}^{Abel} (Abelian part) is defined by the Abelian 3Q Wilson loop $W_{3Q} [u_\mu]$ in the MA gauge,

$$V_{3Q}^{\text{Abel}} = -\lim_{t \rightarrow \infty} \frac{1}{t} \ln \langle W_{3Q} [u_\mu] \rangle. \quad (3.3)$$

Figure 3(a) shows the 3Q potential V_{3Q} and its Abelian part V_{3Q}^{Abel} plotted against the total flux-tube length L_{\min} in SU(3) lattice QCD at $\beta=5.8$ on $16^3 \times 32$ with 2,000 gauge configurations [10]. The Abelian part V_{3Q}^{Abel} of the 3Q potential also takes the Y-Ansatz [10],

$$V_{3Q}^{\text{Abel}} = -\sum_{i < j} \frac{A_{3Q}^{\text{Abel}}}{|\mathbf{r}_i - \mathbf{r}_j|} + \sigma_{3Q}^{\text{Abel}} L_{\min} + C_{3Q}^{\text{Abel}} = -\frac{A_{3Q}^{\text{Abel}}}{R} + \sigma_{3Q}^{\text{Abel}} L_{\min} + C_{3Q}^{\text{Abel}}, \quad (3.4)$$

with $1/R \equiv \sum_{i < j} 1/|\mathbf{r}_i - \mathbf{r}_j|$. At long distances, V_{3Q} and V_{3Q}^{Abel} are almost single-valued functions of L_{\min} , although their multi-valued feature due to the R -dependence is more visible at short distances on finer lattices at $\beta = 6.0$. From Fig.3(a), we find *perfect Abelian dominance* also for the 3Q confinement force, i.e., $\sigma_{3Q}^{\text{Abel}} \simeq \sigma_{3Q} \simeq \sigma$.

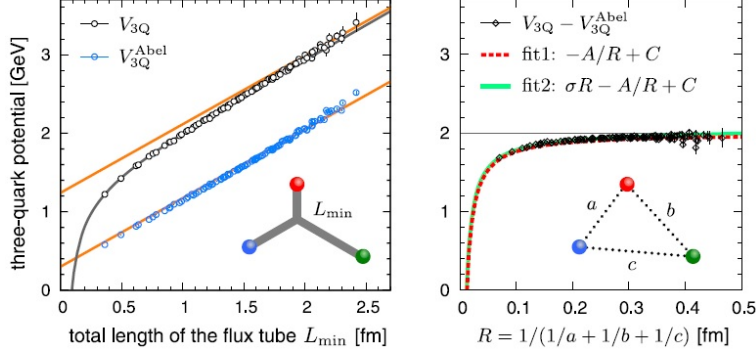


Figure 3: (a) The 3Q potential V_{3Q} (black) and its Abelian part V_{3Q}^{Abel} (blue) plotted against L_{\min} in SU(3) lattice QCD at $\beta=5.8$ on $16^3 \times 32$. We add the best-fit Y-Ansatz curve of the equilateral 3Q case for V_{3Q} and V_{3Q}^{Abel} , respectively. (b) $\Delta V_{3Q} \equiv V_{3Q} - V_{3Q}^{\text{Abel}}$ plotted against R . ΔV_{3Q} can be fit with the pure Coulomb Ansatz (3.4) with no string tension, which indicates $\sigma_{3Q} \simeq \sigma_{3Q}^{\text{Abel}}$. These figures are taken from Ref.[10].

To demonstrate $\sigma_{3Q}^{\text{Abel}} \simeq \sigma_{3Q}$, we show in Fig.3(b) the difference $\Delta V_{3Q} \equiv V_{3Q} - V_{3Q}^{\text{Abel}}$ plotted against R [10], because, if $\sigma_{3Q}^{\text{Abel}} = \sigma_{3Q}$, ΔV_{3Q} is well reproduced by the pure Coulomb Ansatz,

$$\Delta V_{3Q} \equiv V_{3Q} - V_{3Q}^{\text{Abel}} = -\frac{\Delta A_{3Q}}{R} + \Delta C_{3Q}, \quad (3.5)$$

with $\Delta A_{3Q} \equiv A_{3Q} - A_{3Q}^{\text{Abel}}$, $\Delta C_{3Q} \equiv C_{3Q} - C_{3Q}^{\text{Abel}}$ and $1/R \equiv \sum_{i<j} 1/|\mathbf{r}_i - \mathbf{r}_j|$. In Fig.3(b), ΔV_{3Q} obeys a pure Coulomb form with no string tension, which is a clear evidence of *perfect Abelian dominance* of quark confinement in baryons: $\sigma_{3Q}^{\text{Abel}} \simeq \sigma_{3Q}$ [10].

To summarize, from the analysis of the accurate lattice QCD data of $V(r)$, $V^{\text{Abel}}(r)$, V_{3Q} and V_{3Q}^{Abel} [9, 10], we find *perfect Abelian dominance* of the string tension in $Q\bar{Q}$ and 3Q potentials: $\sigma \simeq \sigma^{\text{Abel}} \simeq \sigma_{3Q} \simeq \sigma_{3Q}^{\text{Abel}}$.

4. Monopole Dominance of Quark Confinement in Mesons and Baryons

Finally, we accurately investigate monopole dominance of quark confinement for both $Q\bar{Q}$ and 3Q systems in SU(3) lattice QCD at $\beta=5.8$ on $16^3 \times 32$ with 2,000 gauge configurations.

4.1 Hodge Decomposition and Monopole Projection

In the MA gauge, it is likely that only Abelian gluon component is essential for the long-distance QCD physics, and infrared QCD can be approximated by Abelian-projected QCD, as is indicated by perfect Abelian dominance of quark confinement.

Abelian-projected QCD in the MA gauge has not only the color-electric current j^μ but also the color-magnetic monopole current k^μ , which topologically appears. In the dual superconductor scenario, the monopole current k^μ is considered to play an essential role to quark confinement. By the Hodge decomposition, the Abelian-projected QCD system can be divided into the monopole part ($k_\mu \neq 0$, $j_\mu = 0$) and the photon part ($j_\mu \neq 0$, $k_\mu = 0$), as schematically illustrated in Fig.4. Then, the importance of the monopole current k^μ can be checked, using the Hodge decomposition.

In the lattice formalism, DeGrand and Toussaint performed the Hodge decomposition [14]. In lattice QCD, the Abelian gluon $\theta_\mu(s) = agA_\mu(s)$ is the exponent in Abelian link-variable,

$$u_\mu(s) = e^{i\theta_\mu(s)} = e^{i\theta_\mu^3(s)T^3 + i\theta_\mu^8(s)T^8} = \text{diag}(e^{i\theta_\mu^{(1)}(s)}, e^{i\theta_\mu^{(2)}(s)}, e^{i\theta_\mu^{(3)}(s)}) \in U(1)^2, \quad (4.1)$$

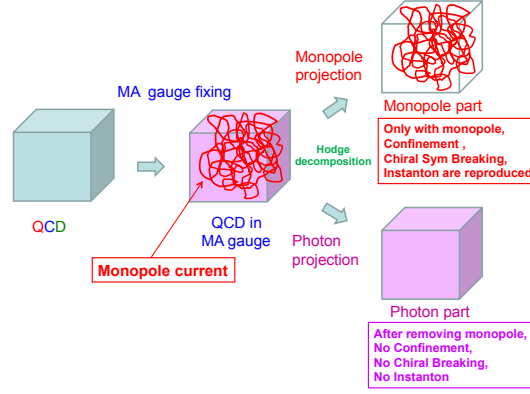


Figure 4: A dual superconductor scenario from QCD in the MA gauge. In the MA gauge, infrared QCD becomes Abelian-like because of large off-diagonal gluon mass of about 1GeV [6], and monopole currents topologically appear [5]. By the Hodge decomposition, the QCD system in the MA gauge can be divided into the monopole part ($k_\mu \neq 0$, $j_\mu = 0$) and the photon part ($j_\mu \neq 0$, $k_\mu = 0$).

with $\theta_\mu^{(i)}(s) \in [-\pi, \pi)$ ($i=1,2,3$), which is consistent with the continuum gluon A_μ as $a \rightarrow 0$. The Abelian field strength $\theta_{\mu\nu}(s) = a^2 g F_{\mu\nu}(s)$ is the exponent in the Abelian plaquette variable,

$$u_{\mu\nu}(s) = e^{i(\partial \wedge \theta)_{\mu\nu}(s)} = e^{i\theta_{\mu\nu}(s)} = e^{i\theta_{\mu\nu}^3(s)T^3 + i\theta_{\mu\nu}^8(s)T^8} = \text{diag}(e^{i\theta_{\mu\nu}^{(1)}(s)}, e^{i\theta_{\mu\nu}^{(2)}(s)}, e^{i\theta_{\mu\nu}^{(3)}(s)}) \in U(1)^2. \quad (4.2)$$

Here, $\theta_{\mu\nu}^{(i)}(s)$ is the principal value $\theta_{\mu\nu}^{(i)}(s) \in [-\pi, \pi)$ ($i=1,2,3$), which is $U(1)^2$ -gauge invariant and consistent with the continuum Abelian field strength $F_{\mu\nu}$ as $a \rightarrow 0$ [4]. Then, $\theta_{\mu\nu}$ is written as

$$\theta_{\mu\nu}(s) = (\partial \wedge \theta)_{\mu\nu}(s) + 2\pi n_{\mu\nu}(s), \quad n_{\mu\nu}^{(i)}(s) \in \mathbf{Z} \quad (i = 1, 2, 3), \quad (4.3)$$

where $n_{\mu\nu}(s)$ is $U(1)^2$ gauge-variant and corresponds to the singular Dirac string as $a \rightarrow 0$ [4]. The electric current j^μ and the monopole current k^μ are derived from the Abelian field strength $\theta_{\mu\nu}$,

$$j_\nu \equiv \partial_\mu \theta_{\mu\nu}, \quad k_\nu \equiv \partial_\mu \tilde{\theta}_{\mu\nu} = 2\pi \partial_\mu \tilde{n}_{\mu\nu}, \quad k_\nu^{(i)} = 2\pi \partial_\mu \tilde{n}_{\mu\nu}^{(i)} \in 2\pi\mathbf{Z}, \quad (4.4)$$

with the dual tensor $\tilde{\theta}_{\mu\nu} \equiv \frac{1}{2} \epsilon_{\mu\nu\alpha\beta} \theta_{\alpha\beta}$. The monopole part θ_μ^{Mo} and the photon part θ_μ^{Ph} satisfy

$$\theta_{\mu\nu}^{\text{Mo}} \equiv (\partial \wedge \theta^{\text{Mo}})_{\mu\nu} \pmod{2\pi}, \quad \partial_\mu \theta_{\mu\nu}^{\text{Mo}} = 0, \quad \partial_\mu \tilde{\theta}_{\mu\nu}^{\text{Mo}} = k_\nu, \quad (4.5)$$

$$\theta_{\mu\nu}^{\text{Ph}} \equiv (\partial \wedge \theta^{\text{Ph}})_{\mu\nu} \pmod{2\pi}, \quad \partial_\mu \theta_{\mu\nu}^{\text{Ph}} = j_\nu, \quad \partial_\mu \tilde{\theta}_{\mu\nu}^{\text{Ph}} = 0. \quad (4.6)$$

From $\partial_\mu \tilde{\theta}_{\mu\nu}^{\text{Ph}} = 0$, one finds $\theta_{\mu\nu}^{\text{Ph}} = (\partial \wedge \theta^{\text{Ph}})_{\mu\nu}$ and $\partial_\mu (\partial \wedge \theta^{\text{Ph}})_{\mu\nu} = \partial^2 \theta_\nu^{\text{Ph}} - \partial_\nu (\partial_\mu \theta_\mu^{\text{Ph}}) = j_\nu$. Taking the Landau gauge $\partial_\mu \theta_\mu^{\text{Ph}} = 0$, the photon part θ_ν^{Ph} is derived from the electric current j_ν ,

$$\partial^2 \theta_\nu^{\text{Ph}} = j_\nu, \quad \theta_\nu^{\text{Ph}} = \frac{1}{\partial^2} j_\nu, \quad \text{i.e.,} \quad \theta_\nu^{\text{Ph}}(s) = \sum_{s'} \langle s | \frac{1}{\partial^2} | s' \rangle j_\nu(s'), \quad (4.7)$$

using the inverse d'Alembertian on the lattice [4]. The monopole part $\theta_\mu^{\text{Mo}}(s)$ is obtained as $\theta_\mu^{\text{Mo}}(s) = \theta_\mu(s) - \theta_\mu^{\text{Ph}}(s)$. The monopole part $\theta_\mu^{\text{Mo}}(s)$ and the photon part $\theta_\mu^{\text{Ph}}(s)$ satisfy Eqs.(4.5) and (4.6) near the continuum with a small a [4].

Using the monopole/photon link-variables,

$$u_\mu^{\text{Mo}}(s) \equiv e^{i\theta_\mu^{\text{Mo}}(s)} \in U(1)^2, \quad u_\mu^{\text{Ph}}(s) \equiv e^{i\theta_\mu^{\text{Ph}}(s)} \in U(1)^2, \quad (4.8)$$

monopole projection and photon projection are defined as follows:

- Monopole projection (the monopole part) is defined by the replacement of $\{u_\mu(s)\} \rightarrow \{u_\mu^{\text{Mo}}(s)\}$, which keeps the monopole current k^μ and eliminates the electric current j^μ .
- Photon projection (the photon part) is defined by the replacement of $\{u_\mu(s)\} \rightarrow \{u_\mu^{\text{Ph}}(s)\}$, which keeps the electric current j^μ and eliminates the monopole current k^μ .

The dominant role of the monopole part is called ‘‘monopole dominance’’, and monopole dominance has been investigated for quark confinement in lattice QCD [8].

4.2 Monopole Dominance of Confinement for Quark-Antiquark and 3Q Systems

The monopole part $V_{\text{Mo}}(r)$ and the photon part $V_{\text{Ph}}(r)$ of the $Q\bar{Q}$ potential are defined by the monopole/photon-projected Wilson loop, $W_{r \times t}[u_\mu^{\text{Mo}}]$ and $W_{r \times t}[u_\mu^{\text{Ph}}]$,

$$V_{\text{Mo}}(r) = -\lim_{t \rightarrow \infty} \frac{1}{t} \ln \langle W_{r \times t}[u_\mu^{\text{Mo}}] \rangle, \quad V_{\text{Ph}}(r) = -\lim_{t \rightarrow \infty} \frac{1}{t} \ln \langle W_{r \times t}[u_\mu^{\text{Ph}}] \rangle. \quad (4.9)$$

Figure 5(a) shows the lattice QCD result for the static $Q\bar{Q}$ potential $V(r)$ in SU(3) QCD, $V_{\text{Abel}}(r)$ in Abelian-projected QCD, $V_{\text{Mo}}(r)$ in the monopole part, and $V_{\text{Ph}}(r)$ in the photon part. While the photon part has almost no confining force, the monopole part almost keeps the confining force. Thus, monopole dominance is found for quark confinement in the $Q\bar{Q}$ system.

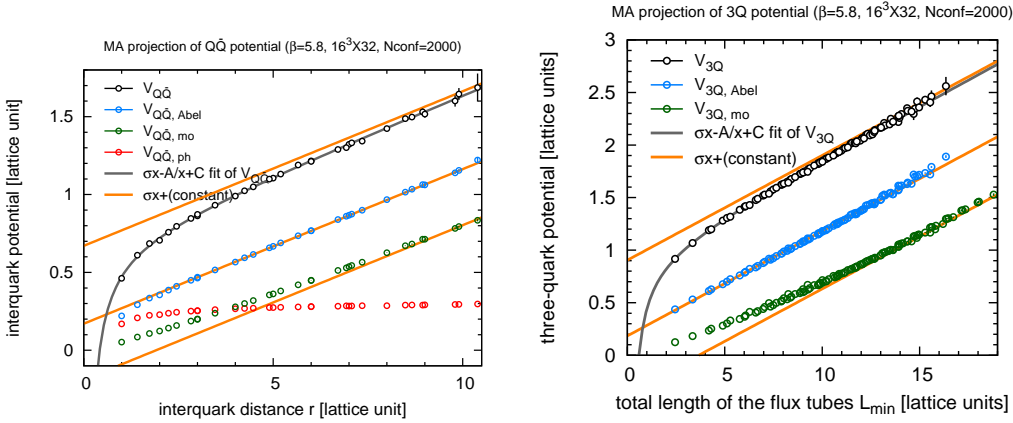


Figure 5: (a) The lattice QCD result for the static $Q\bar{Q}$ potential $V(r)$ (black) in SU(3) QCD, $V_{\text{Abel}}(r)$ (blue) in Abelian-projected QCD, $V_{\text{Mo}}(r)$ (green) in the monopole part, and $V_{\text{Ph}}(r)$ (red) in the photon part. (b) The lattice QCD result for the 3Q potential V_{3Q} (black) in SU(3) QCD, V_{3Q}^{Abel} (blue) in Abelian-projected QCD, and V_{3Q}^{Mo} (green) in the monopole part, plotted against L_{min} .

Similarly, the monopole part $V_{3Q}^{\text{Mo}}(r)$ of the 3Q potential is defined by

$$V_{3Q}^{\text{Mo}} = -\lim_{t \rightarrow \infty} \frac{1}{t} \ln \langle W_{3Q}[u_\mu^{\text{Mo}}] \rangle. \quad (4.10)$$

Figure 5(b) shows the lattice QCD result for the 3Q potential V_{3Q} in SU(3) QCD, V_{3Q}^{Abel} in Abelian-projected QCD, and V_{3Q}^{Mo} in the monopole part, plotted against L_{min} . Monopole dominance is found also for quark confinement in the 3Q system.

The string tension σ_{Mo} in the monopole part is estimated from the lattice QCD data in Fig.5, and monopole dominance is estimated as $\sigma_{\text{Mo}} \simeq 0.92\sigma$ for the string tension in $Q\bar{Q}$ and 3Q systems.

5. Summary and concluding remarks

We have investigated Abelian dominance and monopole dominance of quark confinement for $Q\bar{Q}$ and $3Q$ systems in $SU(3)$ quenched lattice QCD in the MA gauge. For large physical-volume lattices with $La \geq 2\text{fm}$, we have found *perfect Abelian dominance* of the string tension for both $Q\bar{Q}$ and $3Q$ systems: $\sigma \simeq \sigma^{\text{Abel}} \simeq \sigma_{3Q} \simeq \sigma_{3Q}^{\text{Abel}}$. We have found monopole dominance of the string tension for both $Q\bar{Q}$ and $3Q$ systems, and have estimated $\sigma_{\text{Mo}} \simeq 0.92\sigma$.

Acknowledgments

H.S. is supported in part by the Grants-in-Aid for Scientific Research [15K05076] from Japan Society for the Promotion of Science. The lattice QCD calculations were done on NEC-SX8R at Osaka University.

References

- [1] Y. Nambu, *Phys. Rev.* **D10**, 4262 (1974); G. 't Hooft, in *High Energy Physics*, (Editorice Compositori, Bologna, 1975); S. Mandelstam, *Phys. Rept.* **23**, 245 (1976).
- [2] G. 't Hooft, *Nucl. Phys.* **B190**, 455 (1981).
- [3] Z. F. Ezawa and A. Iwazaki, *Phys. Rev.* **D25**, 2681 (1982).
- [4] H. Ichie and H. Suganuma, *Nucl. Phys.* **B548**, 365 (1999); *Nucl. Phys.* **B574**, 70 (2000); H. Suganuma, H. Ichie, A. Tanaka and K. Amemiya, *Prog. Theor. Phys. Suppl.* **131**, 559 (1998).
- [5] A. S. Kronfeld, G. Schierholz and U.-J. Wiese, *Nucl. Phys.* **B293** 461 (1987); A. S. Kronfeld, M. L. Laursen, G. Schierholz and U.-J. Wiese, *Phys. Lett.* **B198**, 516 (1987).
- [6] K. Amemiya and H. Suganuma, *Phys. Rev.* **D60**, 114509 (1999); S. Gongyo and H. Suganuma, *Phys. Rev.* **D87**, 074506 (2013); S. Gongyo, T. Iritani and H. Suganuma, *Phys. Rev.* **D86**, 094018 (2012).
- [7] T. Suzuki and I. Yotsuyanagi, *Phys. Rev.* **D42**, 4257(R) (1990).
- [8] J. D. Stack, S. D. Neiman and R. J. Wensley, *Phys. Rev.* **D50**, 3399 (1994).
- [9] N. Sakumichi and H. Suganuma, *Phys. Rev.* **D90**, 111501(R) (2014).
- [10] N. Sakumichi and H. Suganuma, *Phys. Rev.* **D92**, 034511 (2015).
- [11] T. T. Takahashi, H. Matsufuru, Y. Nemoto and H. Suganuma, *Phys. Rev. Lett.* **86**, 18 (2001); T. T. Takahashi, H. Suganuma, Y. Nemoto and H. Matsufuru, *Phys. Rev.* **D65**, 114509 (2002); T. T. Takahashi and H. Suganuma, *Phys. Rev. Lett.* **90**, 182001 (2003); *Phys. Rev.* **D70**, 074506 (2004).
- [12] N. Brambilla, J. Ghiglieri and A. Vairo, *Phys. Rev.* **D81**, 054031 (2010); N. Brambilla, F. Karbstein and A. Vairo, *Phys. Rev.* **D87**, 074014 (2013).
- [13] H. Ichie, V. Bornyakov, T. Streuer and G. Schierholz, *Nucl. Phys.* **A721**, 899 (2003); V. G. Bornyakov *et al.* (DIK Coll.), *Phys. Rev.* **D70**, 054506 (2004); *Phys. Rev.* **D70**, 074511 (2004).
- [14] T. A. DeGrand and D. Toussaint, *Phys. Rev.* **D22**, 2478 (1980).